Encephalic NMR Tumor Diversification by Textural Interpretation

Danilo Avola and Luigi Cinque

University of Rome "La Sapienza", Department of Computer Science
Via Salaria 113, 00198 Rome, Italy
{avola,cinque}@di.uniroma1.it
http://w3.uniroma1.it/dipinfo/english/index.asp

Abstract. The novel technologies used in different application domains allow to obtain digital images with a high complex informative content. These meaningful information are expressed by textural skin that covers the objects represented inside the images. The textural information can be exploited to interpret the semantic meaning of the images themselves. This paper provides a mathematical characterization, based on texture analysis, of the craniopharyngioma pathology distinguishing it from other kinds of primary cerebral tumors. By this characterization a prototype has been developed, which has primarily allowed to identify potential abnormal masses inside the cerebral tissue and subsequently to possibly classify them as craniopharyngiomas.

Keywords: Medical image, texture analysis, pattern recognition, feature extraction, segmentation, classification, co-occurrence matrix.

1 Introduction

The novel image capture devices used in the different application domains allow to obtain images with high level details. These images often possess an informative content that goes beyond the simple visual representation. That is, by observing the relationships between pixels or clusters of pixels (that is, the texture) of the objects inside the images, it is possible to bring out the meaningful features through which to describe the semantic informative content of the images. In the last years, there have been many efforts to adopt the image analysis processes on medical images. The reason for this, comes from the need to get intelligent and automated systems for carrying out, in real time, several critical duties, such as: diagnosis, analysis, zones delineation, abnormal masses identification and irradiation, and so on. The making of these systems is still a hard task, and the current Decision Support Systems (DSSs) are still scanty tools.

This paper provides a concrete advancement of our results just shown in [1]. In particular, our previous work provided the numerical characterization, based on texture analysis, of each object represented in the NMR encephalic images (cerebral tissue, rest of skull, possible abnormal mass, and background). The step ahead of this paper has been to provide a further numerical class able to

P. Foggia, C. Sansone, and M. Vento (Eds.): ICIAP 2009, LNCS 5716, pp. 394–403, 2009.

distinguish the craniopharyngioma pathology from other kinds of primary cerebral tumors. There is an extensive heterogeneous literature on medical images analysis focalized on different aspects of medical image processing, such as: image segmentation, masses detection, and so on. In particular, these approaches are based on several principles related to the image understanding, but no so much works tend to exploit totally the morphological structure (given by texture analysis) of the objects inside the biomedical images, moreover there is no works about concrete mathematical characterization of a specific NMR brain tumor. In [2] an interesting approach of medical image processing is given, in particular the authors present a framework for multiple object segmentation in medical images that respects the topological properties and relationships of structures as given by a template. In [3] another framework for the segmentation of brain magnetic resonance imaging (MRI) is given. In particular, the authors provide an approach that combines atlas registration, fuzzy connectedness (FC) segmentation, and parametric bias field correction (PABIC) to perform automatically the segmentation task. A complex medical image processing system is shown in [4], in this work the authors present an approach, based on evolutionary computing, to medical image segmentation. In this approach the segmentation task, on sagittal brain magnetic resonance images (MRI), has been reached by complementing the image-pixel integration power of deformable shape models with the high-level control mechanisms of genetic algorithms (GAs). Diversely, the common approaches, such as [5], aim to exploit the well known features of the image content, such as: edge detection, boundary detection, model correlation-based, region-based, and so on. An alternative approach is also proposed in [6], in this approach the texture modeling is based on the implicit incorporation of spatial information through the introduction of particular matrixes that take into account the spatial relationships among pixels. Another interesting approach is proposed in [7], where the application, based on random neural network, accomplishes the texture classification and retrieval. In particular, in this context a neuron in the network corresponds to an image pixel and the neurons are connected according to neighboring relationship between pixels. In this way, a texture can be represented with the weights of the network. In [8] the authors give a last remarkable framework through which to perform brain MRI segmentation. In this approach the segmentation is performed by applying nonparametric density estimation, using the mean shift algorithm in the joint spatial-range domain.

Unlike the previous works, the proposed approach provides the identification of a well defined mathematical characterization, texture based, of the morphological structure of the craniopharyngioma pathology inside the encephalic NMR images. The paper is organized as follows. Section 2 introduces both the proposed image processing methodology and the numerical class representing the primary cerebral tumors. Section 3 introduces the numerical class about the craniopharyngioma pathology. Section 4 summarizes the medical cases study. Finally, Section 5 concludes.

2 Methodology and Designed Architecture

In order to determine the mathematical characterization related to the craniopharyngioma pathology (shown in the next section) we have exploited the classification obtained in our previous work [1]. Besides, also the adopted methodology as well as the used prototype coming from the same work. For this reason, this section shows the main aspects of the mentioned work.

With the purpose to obtain the preliminary textural mathematical characterization of the cerebral tissue necessary to subsequently distinguish craniopharyngioma pathology from other kinds of primary cerebral tumors has been adopted the methodology shown in Figure 1. Each one of the three modules will now be briefly explained.

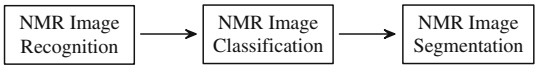

Fig. 1. Methodology: the three modules

The recognition phase, applied on selected NMR images (chosen transversal T_1 weighted, with or without contrast) is designed to perform feature extraction activity on the following fix objects: object 1: possible cerebral anomaly (i.e.: primary cerebral tumor), object 2: cerebral tissue, object 3: rest of the image (i.e.: muscular and bony structure), object 4: background.

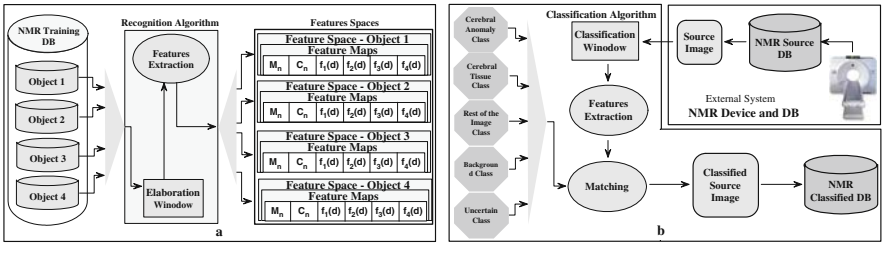

Fig. 2. Architecture: a) recognition phase b) classification phase

As shown in Figure 2-a, four different databases each one containing some images representing a collection of the same kind of objects have been used as training database. The feature extraction process has been performed by a preestablished elaboration window within which the feature extraction algorithm, based on textural statistical operators, worked to catch the different textural features. At the end of the recognition phase every image (in every database) provided several feature maps, these sets of feature maps, according to the specific objects, have constituted the feature spaces through which to provide the

mathematical characterization of the objects themselves. The six textural statistical operators chosen to extrapolate the semantic meaning of the texture have been selected from the first and second order statistical class [9].

The operators belonging to the first order statistical class are: *N-Order Moment* (M_n) and *M-Order Central Moment* (C_m):

$$M_n = \sum_{i=0}^{N} i^n \times p(i), C_m = \sum_{i=0}^{N} (i - M_1)^m \times p(i) \tag{1}$$

Where: *p(i)* represents the probability that the gray level value i appears inside the elaboration window (E.W.). The following constraints must be respected:

$$0 \leq p(i) \leq 1 \ \forall i \in [0..255] \subset \mathrm{N}, \sum_{i=0}^{N} p(i) = 1, N = 255, n = 1, m = 2 \tag{2}$$

The remaining chosen four operators, co-occurrence matrix based, work according to the principle scheme shown in Figure 3.

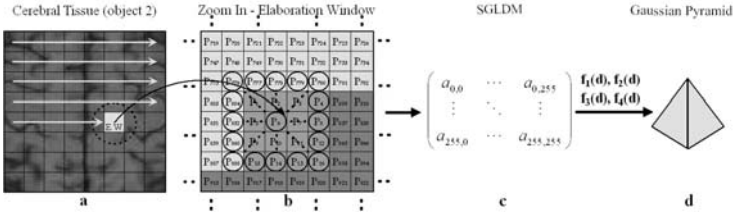

Fig. 3. NMR texture operators principle scheme

Figure 3-a represents the scanning (by Elaboration Window, E.W.) of an image belonging to sub-database object 2. Every square zone, where the arrow appears, identifies an elaborated image zone. The E.W. identifies the image zone under processing. The remaining image zones will be processed after the "actual" E.W.. In Figure 3-b can be observed that each pixel making up the elaboration window ($P_1..P_{16}$) will be considered as "the centre" of a "circle" whose radius value is predefined (called "d"). Every couple of points (centre point and each one on the boundary of the circumference) will increase by one frequency its coefficient on the co-occurrence matrix, Figure 3-c, at the coordinates (*row*, *column*) $a_{m,n}$ fixed through the gray tone level of considered points. The Figure 3-d shows the new image (feature map) that results after the full scanning.

Every E.W. that processes the image in Figure 3-a gives back (by the different operators) a single pixel that makes up the feature map. Thus, every feature map is sub-sampled (depending on the considered E.W. size) referring to the original image. This process can be repetitively performed on the obtained image. This working method is defined as "Gaussian Pyramidal Approach" [10], where

every obtained image represents a level of the pyramid (original image is the pyramid base). Our approach considers, for every image in the whole NMR training DB two levels of the Gaussian Pyramid (L_0 and L_1). Also the two operators, belonging to the first order statistics, exploit the pyramidal approach.

The mentioned operators, belonging to the second order statistical class, are: *Homogeneity* ($f_1(d)$), *Contrast* ($f_2(d)$), *Inverse Difference* ($f_3(d)$), and *Entropy* ($f_4(d)$):

$$\begin{aligned} f_1(d) &= \sum_{i=0}^{N}\sum_{j=0}^{N}\left[p_d(i,j)\right]^2, f_2(d) = \sum_{i=0}^{N}\sum_{j=0}^{N}(i-j)^2\left[p_d(i,j)\right]^l \\ f_3(d) &= \sum_{i=0}^{N}\sum_{j=0}^{N}\frac{\left[p_d(i,j)\right]^l}{1+(i-j)^k}, f_4(d) = -\sum_{i=0}^{N}\sum_{j=0}^{N}p_d(i,j)\log_n(p_d(i,j)) \end{aligned} \tag{3}$$

Where: $p_d(i,j)$ represents the probability that two points with distance "d" have respectively i and j gray value. The following constraints must be respected:

$$\begin{aligned} &0 \leq p_d(i,j) \leq 1, \forall(i,j) \in [0....255] \times [0....255] \subset \mathrm{N}^2 \\ &\sum_{i=0}^{N}\sum_{j=0}^{N}p_d\,(i,j) = 1\,, N = 255,\, k = 2,\, l = 1,\, n = 2 \end{aligned} \tag{4}$$

The operators ($f_1(d)$, $f_2(d)$), belonging to the Computer Vision (CV), are exploited to emulate human textural visual perception of two main parameters used by human analyst during NMR analysis: homogeneity and contrast. The operators ($f_3(d)$, $f_4(d)$) belonging to the Information Retrieval (IR) techniques, complete the feature extraction work. All four mentioned operators have been used with two different distance values "d" (d = 2, 3).

With the purpose of explaining both the way the mathematical classes have been built and how the original NMR images coming from the device have been classified, in Figure 2-b is shown the detailed software architecture of the NMR classification phase. In this phase, the feature spaces of each object (provided by recognition phase) have been carefully analyzed by grey tones histogram and correlated to others feature spaces belonging to the same objects. In this way four univocal mathematical characterizations, called *classes*, have been accomplished. As consequence, a class called *uncertain* is made up. It contains all those pixel configurations that are not included in the *classes*.

In this section (Figure 4-a) is shown only the mathematical class related to the possible cerebral anomaly (i.e.: primary cerebral tumors). The functions M_1, C_2, $f_1(d)$, $f_2(d)$, $f_3(d)$, and $f_4(d)$ are the operators used into the E.W. (where d = 2, 3). Moreover T_i, for $0 \leq i \leq 30$, are the extrapolation constants fixed to the following grey tone intensity values: $T_0..T_{30}$: 97, 18, 193, 33, 55, 140, 186, 8, 107, 120, 255, 55, 88, 121, 164, 6, 39, 70, 220, 25, 33, 71, 101, 198, 248, 110, 165, 80, 110, 45, 65. In Figure 5-a a visual example of the classes is shown.

The shown result is only related to the first level of the Gaussian Pyramid (L_0) (our algorithm takes into account (L_0) and (L_1)). In fact, this level represents the basic feature to distinguish the cerebral anomaly class from the other three *classes* (cerebral tissue class, rest of the image class, background class). By the

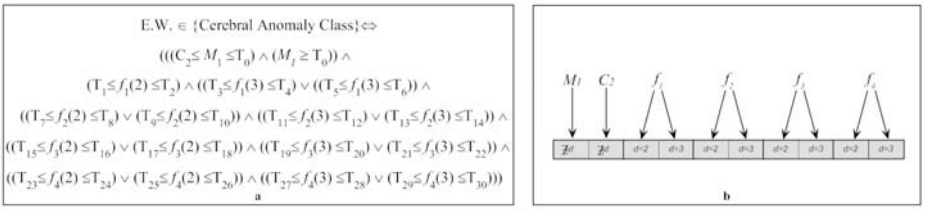

Fig. 4. a) Cerebral anomaly class b) Feature vector

formalized *classes* it is possible to explain how the original NMR images coming from the device have been classified.

As shown in Figure 2-b, the source images coming directly from the nuclear magnetic resonance device (NMR source database) are directly scanned, by a classification window (C.W. of the same size of the E.W.), in the same way as in the recognition phase. From each C.W. on these images a feature vector is extrapolated (features extraction). This vector, as shown in Figure 4-b, regards the same measures (operators) used for the recognition phase (with L_0 and L_1 levels). Each single feature vector, extracted from the original image, tries the matching (in the matching module) to the formalized classes. After the right class has been found, that particular cluster is assigned to the related class. After all source image clusters have been considered the image areas belonging to the same formalized classes are joined together. At the end of this process the outcome is that each zone of each image is classified as belonging to one of four formalized classes or (for exclusion) belonging to the *uncertain* class. Every classified image is arranged in the new database (NMR classified DB).

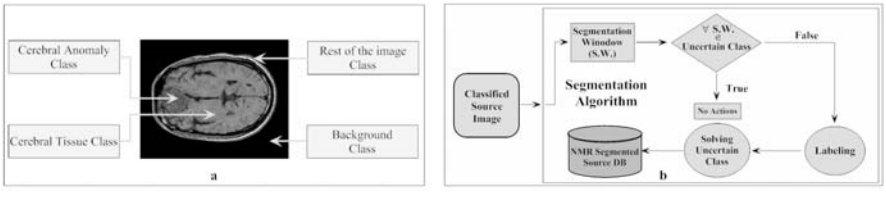

Fig. 5. a) Main classes b) Architecture: segmentation phase

The segmentation phase represents the last step of our image analysis process. In this phase two main tasks are accomplished. In the first a simple labeling process is performed on the classified source image. In the second the system solves all these image zones that belong to the *uncertain* class.

In Figure 5-b is shown the segmentation phase architecture. Each classified source image is directly scanned by a segmentation window (S.W. of the same size of C.W. and E.W.). As shown in Figure 5-b, if the pixels into the S.W. belong to one formalized class then all the pixels into the S.W. will be suitably

labeled. Otherwise, no action is performed, and the system scans next S.W.. At the end of this first step a large amount of the image is labeled. In the second step, the unlabeled image zones are solved. The image zones belonging to the *uncertain* class are subdivided in two categories: not recognized zones (NRZs), spurious zones (SZs). Primarily, by context based algorithm, the first kind of ambiguity is solved. Subsequently, by decisional algorithm, also the second kind of ambiguity is solved. At the end of segmentation process every source image is perfectly labeled and arranged in NMR segmented source DB.

3 Craniopharyngioma Class

Once obtained the cerebral anomaly class (and related image segmentation), the framework can detect, as shown in Figure 6, the presence of abnormal masses inside the cerebral tissue. But it is not able to identify the kind of primary cerebral tumor.

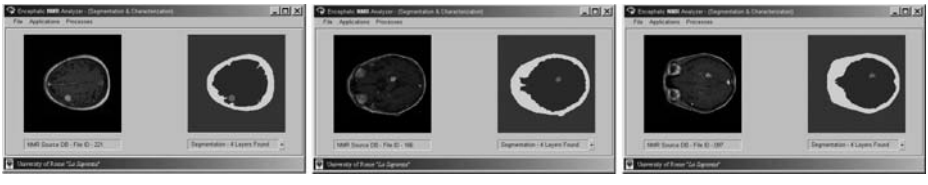

Fig. 6. Examples of detected primary cerebral tumors

The concrete advancement of the proposed work has been to distinguish the craniopharyngiomas pathology from other kinds of primary cerebral tumors. The first step to accomplish this task has been to find other textural statistical operators able to extrapolate the morphological structure of the texture expressed from the craniopharyngiomas tissue. Experimental observations have enabled to select, always belonging to the second order statistical class, the following two operators: *Correlation* ($f_5(d)$), *Difference Entropy* ($f_6(d)$):

$$f_5(d) = \sum_{i=0}^{N}\sum_{j=0}^{N} \frac{(i-\mu_x)(j-\mu_y)p_d(i,j)^l}{[\sigma_x\sigma_y]^m}, f_6(d) = -\sum_{i=0}^{N} p_{x-y}(i)\log_n[p_{x-y}(i)] \qquad (5)$$

Where:

$$\begin{aligned} \mu_x &= \sum_{i=0}^{N}\sum_{j=0}^{N} i\left(p_d(i,j)\right), \sigma_x = \sqrt{\sum_{i=0}^{N}\sum_{j=0}^{N}(i-\mu_x)^2\left(p_d(i,j)\right)} \\ \mu_y &= \sum_{i=0}^{N}\sum_{j=0}^{N} j\left(p_d(i,j)\right), \sigma_y = \sqrt{\sum_{i=0}^{N}\sum_{j=0}^{N}(i-\mu_y)^2\left(p_d(i,j)\right)} \\ p_{x-y}(k) &= \sum_{i=0}^{N}\sum_{j=0}^{N}[p_d(i,j)]^q, where|i-j| = k \end{aligned} \qquad (6)$$

Obviously, $p_d(i, j)$ has the same meaning and has to respect the the same constraints shown in the previous section. Moreover, experimental observations have fixed, on the two mentioned operators, the following parameters: $l = 1$, $m = 1$, $n = 2$, $q = 1$. More specifically, these two operators have been selected according to their capacity to catch both micro structural changes on texture with low level of stationarity and macro morphological pattern on texture with high level of entropy.

The two statistical operators ($f_5(d)$, $f_6(d)$) have been used, by the methodology and the algorithms explained in the previous section, on the zones of images recognized as belonging to the cerebral anomaly class. In particular, the operators have been used with three different distance values "d" (d = 1, 2, 3). In this way, it has been possible to distinguish, within the cerebral anomaly class, the sub-class craniopharyngioma, as shown in Figure 7-a (it is shown only the results related to the first level of the Gaussian Pyramid (L_0)). In Figure 7-b is also shown the related feature vector.

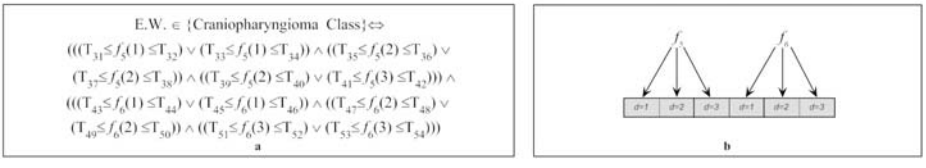

Fig. 7. a) Craniopharyngioma class. b) Feature vector

The functions $f_5(d)$, $f_6(d)$ are the operators used into the E.W. (where d = 1, 2, 3). Moreover T_i, for $31 \leq i \leq 54$, are the extrapolation constants fixed to the following grey tone intensity values: $T_{31}..T_{54}$: 25, 145, 198, 255, 33, 180, 220, 250, 23, 109, 148, 213, 70, 112, 160, 200, 34, 57, 100, 127, 110, 200, 220, 255.

4 Experimental Results

This section shows both the cases study through which the craniopharyngioma class has been built (NMR image recognition) and the case studies for the experimental phase (NMR image classification and segmentation).

The whole image set was made up of 1015 images provided by 255 selected patients. As in our previous work, the patients have been selected by a protocol in which was specified rules for patients inclusion or exclusion. Moreover, the protocol also specified particular texture requirements able to discard images where objects were represented by messy and/or ambiguous patterns of pixels. The main aim of the protocol was to avoid the introduction of unknown texture caused by several factors, such as: brain prostheses, recent brain operations, and so on.

All the used images have been selected according to the encephalic NMR diagnostic standard: depth 8 bit gray-scale, spatial resolution 512x512 pixels.

Table 1. Cases Study

Total Patients	Training DB		Source DB			Total Images
	CRF Patients	3/5 images	PCT Patients (42% CRF patients)	3/5 images 415		
255				CRF Patients	PCT Patients	1015
	150	600	105	175	240	

With these images the training DB and source DB have been built. In the Table 1 a short description case studies is shown. The total patients (255) have been subdivided into two groups: a first group (training DB) made up from 150 craniopharyngioma patients and the second group (source DB) made up from 105 primary cerebral tumor patients. The 42% of the patients belonging to the second group was affected by craniopharyngioma pathology. From each patient of the first and second group have been chosen respectively from 3 to 5 images (600 total images shown craniopharyngioma pathology), and from 3 to 5 images (415 total images, of which 175 shown craniopharyngioma pathology and 240 shown another kind of primary cerebral tumors).

Using the two classes shown in this work, our prototype has almost always correctly classified a craniopharyngioma pathology (success rate: 93%). In the remaining 7% of cases, the prototype always detected the presence of a primary cerebral tumor, but it failed during the classification process. The images for which the prototype fails have both a real small portion of pixel related the craniopharyngioma pathology and their position is almost ambiguous. This problem should be solved by using a whole set of images of a specific patient, and/or by enriching the operators used to define the craniopharyngioma class.

We have observed that the craniopharyngioma classification is reasonably independent from the height of the NMR scanning plan. Moreover, in the worst case, the difference between the real size of the craniopharyngioma pathology in the source image and the size of the labeled related object in the segmented image is about 9%.

5 Conclusion

This paper provides a mathematical characterization, based on texture analysis, of the craniopharyngioma pathology distinguishing it from other kinds of primary cerebral tumors. The developed prototype has shown the effectiveness of the obtained results.

By using all image categories (T_1, T_2, proton density, flair) and all scanning anatomic planes (sagittal, frontal, transversal) could be obtained several recognition/classification improvements, which should be aim to relax constraints of the protocol used to select patients and their images. More specifically, the prototype needs of a new advanced experimental session on a not controlled diagnostic environment.

The proposed approach can be also exploited to reach further advanced targets in NMR image analysis, such as: identification and classification of other kinds of primary cerebral tumors, 3D textural reconstruction, textural modeling of the brain and so on.

References

1. Avola, D., Cinque, L.: Encephalic NMR Image Analysis by Textural Interpretation. In: Proceedings of the 2008 ACM Symposium on Applied Computing, SAC 2008, pp. 1338–1342. ACM Press, New York (2008)
2. Bazin, P.L., Pham, D.L.: Topology Correction of Segmented Medical Images Using a Fast Marching Algorithm. Comput. Methods Prog. Biomed. 88(2), 182–190 (2007)
3. Zhou, Y., Bai, J.: Atlas-Based Fuzzy Connectedness Segmentation and Intensity Nonuniformity Correction Applied to Brain MRI. IEEE Transactions on Biomedical Engineering 54(1), 122–129 (2007)
4. McIntosh, C., Hamarneh, G.: Genetic Algorithm Driven Statistically Deformed Models for Medical Image Segmentation. In: ACM Workshop on Medical Applications of Genetic and Evolutionary Computation Workshop, MedGEC 2006, p. 8. ACM Press, New York (2006)
5. Yan, P., Kassim, A.A.: Medical Image Segmentation Using Minimal Path Deformable Models with Implicit Shape Priors. IEEE Transactions on Information Technology in Biomedicine 10(4), 677–684 (2006)
6. Zwiggelaar, R., Blot, L., Raba, D., Denton, E.R.E.: Set-Permutation-Occurrence Matrix Based Texture Segmentation. In: Perales, F.J., Campilho, A.C., Pérez, N., Sanfeliu, A. (eds.) IbPRIA 2003. LNCS, vol. 2652, pp. 1099–1107. Springer, Heidelberg (2003)
7. Teke, A., Atalay, V.: Texture Classification and Retrieval Using the Random Neural Network Model. Journal on Computational Management Science 3(3), 193–205 (2006)
8. Jimenez-Alaniz, J.R., Medina-Banuelos, V., Yanez-Suarez, O.: Data-Driven Brain MRI Segmentation Supported on Edge Confidence. IEEE Trans. Med. Imaging 25(1), 74–83 (2006)
9. Julesz, B.: Dialogues on Perception. Bradford/MIT Press, Cambridge (1995)
10. Heeger, D.J., Bergen, J.R.: Pyramid-Based Texture Analysis/Synthesis. In: Proceedings of the 22nd Annual Conference on Computer Graphics and Interactive Techniques, SIGGRAPH 1995, pp. 229–238. ACM Press, New York (1995)